Experimental and Theoretical Studies on the Reactions of Aliphatic Imines with Isocyanates

Author(s):
Cotter, Etienne; Pultar, Felix; Riniker, Sereina; Altmann, Karl-Heinz

Publication date:
2024-03-07

Permanent link:
https://doi.org/10.3929/ethz-b-000658270

Originally published in:
Chemistry - A European Journal 30(14), https://doi.org/10.1002/chem.202304272

Chemistry–A European Journal
Research Article
doi.org/10.1002/chem.202304272
Chemistry Europe
European Chemical Societies Publishing
www.chemeurj.org

Experimental and Theoretical Studies on the Reactions of Aliphatic Imines with Isocyanates

Etienne Cotter,[a] Felix Pultar,[b] Sereina Riniker,[b] and Karl-Heinz Altmann*[a]

In the context of a project aiming at the replacement of the 3-substituted β-lactam ring in classical β-lactam antibiotics by an N(3)-acyl-1,3-diazetidinone moiety, we have investigated the reaction of isocyanates with imines derived from allyl glycinate and differently substituted propionaldehydes. Imines of aromatic aldehydes with anilines have been reported to react with acyl isocyanates to give 1,3-diazetidinones or 2,3-dihydro-4*H*-1,3,5-oxadiazin-4-ones, *via* [2+2] or [4+2] cycloaddition, respectively. However, neither of these products was formed with imines derived from allyl glycinate and 2-(mono)methyl propionaldehydes. α,α-Dimethylation of the imine enabled the [4+2] cycloaddition pathway, but the desired 1,3-diazetidinone products were not observed. Surprisingly, the imines obtained from thioesters of 2,2-dimethyl 3-oxo propionic acid reacted with aryl isocyanates or with benzyl isocyanate to give 5,5-dimethyl-2,4-dioxo-6-(aryl-/alkylthio)tetrahydropyrimidines, *via* thiol displacement and re-addition to a putative six-membered iminium intermediate. These experimental results obtained for the reactions could be rationalized by DFT calculations. In addition, we have shown that N(3)-acyl-1,3-diazetidinone and 2,3-dihydro-4*H*-1,3,5-oxadiazin-4-one products can be distinguished based on experimental IR data in combination with theoretical reference spectra employing the IR spectra alignment (IRSA) algorithm. This discrimination was not possible by means of ^{1}H, ^{13}C, or ^{15}N NMR spectroscopy

Introduction

The emergence of antimicrobial resistance (AMR) poses one of the major global health problems for the coming decades.[1–3] To meet this threat, the development of new antibiotics is urgently required; ideally, these drugs should be based on new structural scaffolds and/or should act on new antibacterial targets in order at least to retard the emergence of resistance.[4,5] Before this background, we have been interested in the synthesis and eventual biological investigation of core-modified analogs **2** of natural-derived β-lactam antibiotics of types **1 a** and **1 b**, where the 3-(acylamino)-β-lactam ring is replaced by an N(3)-acylated 1,3-diazetidinone moiety (Figure 1).

Compounds **2** were conceived based on the hypothesis that they could still react with and inactivate penicillin-binding proteins (PBPs)[6] but would also act as covalent reversible inhibitors of β-lactam-inactivating serine β-lactamases (classes A, C and D).[7] Inactivation would be due to the formation of a less hydrolytically susceptible carbamate upon reaction with the active site serine.[8,9] These general concepts have been previously advocated by others[10–17] and their possible viability is supported by some computational[10–15] as well as a limited set of experimental data.[17] However, none of these previous studies has included analogs bearing acyl substituents on N(3) of the 1,3-diazetidinone ring, which we considered important in

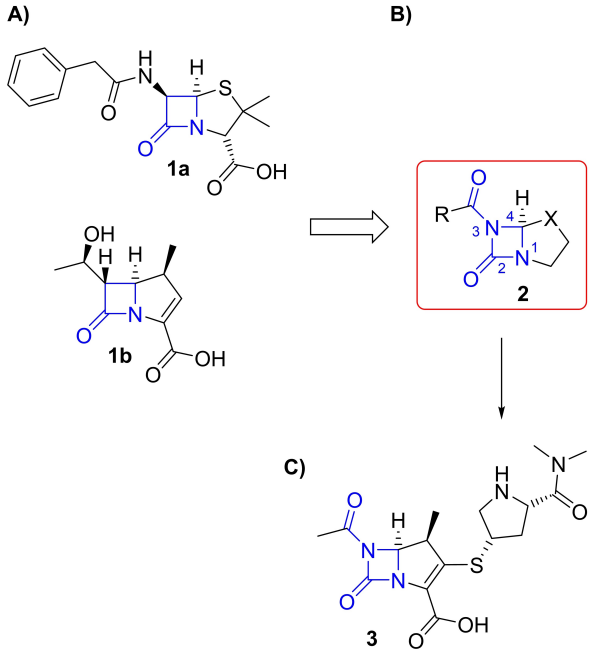

Figure 1. A) Structures of penicillin G (**1 a**) and meropenem (**1 b**) as examples of prototypical β-lactam antibiotics. B) General structure of diazetidinone-based β-lactam analogs. C) Structure of meropenem analog **3**.

[a] *E. Cotter, Prof. Dr. K.-H. Altmann*
Department of Chemistry and Applied Biosciences
Institute of Pharmaceutical Sciences, ETH Zürich
Vladimir-Prelog-Weg 4, 8093 Zürich, Switzerland
E-mail: karl-heinz.altmann@pharma.ethz.ch

[b] *Dr. F. Pultar, Prof. Dr. S. Riniker*
ETH Zürich, Department of Chemistry and Applied Biosciences
Institute of Molecular Physical Science
8093 Zürich, Switzerland

Supporting information for this article is available on the WWW under https://doi.org/10.1002/chem.202304272

order to enhance the reactivity of the urea type endocyclic carbonyl group in 1,3-diazetidinones. The specific target structure chosen to assess the concept outlined above, based on a combination of synthetic and bioactivity considerations, was 1,6-diazabicyclo[3.2.0]hept-2-en-7-one derivative **3**, which is related to meropenem (Figure 1).

Synthetically, the N-acyl 1,3-diazetidinone system in meropenem analog **3** was thought to be accessible *via* [2+2] cycloaddition of an acyl isocyanate with an appropriate imine, based on earlier studies by Arbuzov and co-workers in the 1960's.[18–20] According to Arbuzov's findings, the reaction of acyl isocyanates with imines can either lead to 1,3-diazetidinones *via* [2+2] cycloaddition or to 2,3-dihydro-4*H*-1,3,5-oxadiazin-4-ones *via* [4+2] cycloaddition, depending on the exact reaction conditions (Scheme 1). Both reactions are believed to proceed *via* a zwitterionic iminium intermediate, which is formed upon attack of the imine nitrogen on the isocyanate carbonyl. This intermediate can then progress either to a four-membered 1,3-diazetidinone or a six-membered dihydro-oxadiazinone depending on the attacking nucleophile (green arrows or red arrows in Scheme 1, respectively). However, no dedicated mechanistic studies, either experimental or computational, have been reported for reactions between acyl isocyanates and imines. The formation of 2,3-dihydro-4*H*-1,3,5-oxadiazin-4-ones has also been observed by Tsuge and co-workers[21,22] and by Neidlein and Bottler,[23] while neither of these groups reported the formation of 1,3-diazetidinones. Although we felt encouraged by Arbuzov's results, we were also cognizant of the fact that all imines investigated in his studies and also those investigated by Tsuge or Neidlein were derived from substituted benzaldehydes (or once from pyridine-2-carboxaldehyde and once from pyridine-4-carboxaldehyde)[21] and anilines. In this paper, we now report on the reactions of acyl isocyanates with a series of imines derived from aliphatic aldehydes and allyl glycinate, which were meant to produce 1,3-diazetidinones that could be further elaborated into **3** or related carbapenem analogs. In addition, we have also studied the reaction of these imines with differently substituted phenyl isocyanates. However, the desired 1,3-diazetidinones were never obtained; instead, the only cycloaddition products observed were those formed *via* a [4+2] reaction pathway. These experimental findings could be rationalized by DFT calculations.

Results and Discussion

Experimental work

As depicted in Scheme 2, meropenem analog **3** was to be obtained from carboxylic acid **4** and thiols **5a** or **5b** according to methodology that has been developed by Kondo and co-workers for the synthesis of 1-β-methylcarbapenems (and that will be discussed in more detail below).[24]

Following the general approach discussed above for the construction of the N(3)-acyl 1,3-diazetidinone moiety, carboxylic acid **4** was envisioned to be accessed from *in situ* generated acetyl isocyanate (**6**) and imine **7** *via* thermal [2+2] cycloaddition followed by TBS-removal and oxidation.

Our synthetic work commenced with the preparation of imine **7** from aldehyde **8**[25] and allyl glycinate (**9**)[26,27] (Scheme 3). Condensation of **8** and **9** in the presence of Et_3N and $MgSO_4$ gave crude **7** in 88% yield (as a 8.3:1 mixture with **8** (11%));[28] while unreacted amine **9** was removed in the aqueous work-up, attempts to remove **8** by silica gel chromatography led to hydrolysis of **7**.

In initial experiments, attempts to react the mixture of **7** and **8** with acetyl isocyanate (**6**) (formed *in situ* from acetamide and $(COCl)_2$)[29] only gave acetyl urea **12** in 20–40% yield together with small amounts of enamide **13** (2–5%) (after aqueous work-up). When commercial benzoyl isocyanate (**10**) was reacted with imine **7**, approximately equal amounts of benzoyl urea **14** and enamide **15** were isolated as an inseparable mixture (42% and 27% chemical yield, respectively; *E/Z*=4:1 for **15**) (Scheme 3); the structures of **12** and **14** were confirmed by X-ray crystallography. Importantly, the reaction of **7** neither with **6** nor with **10** produced any detectable amounts of the desired diazetidinones **16** or **17**, respectively.

Several explanations are possible for the formation of ureas **12** and **14**: (1) The presence of residual amine **9** in the imine material (*vide supra*) would directly lead to urea formation by

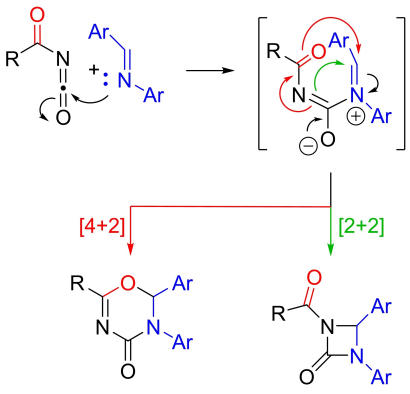

Scheme 1. Possible pathways for the reaction of acyl isocyanates with imines according to Arbuzov and co-workers.[18,19]

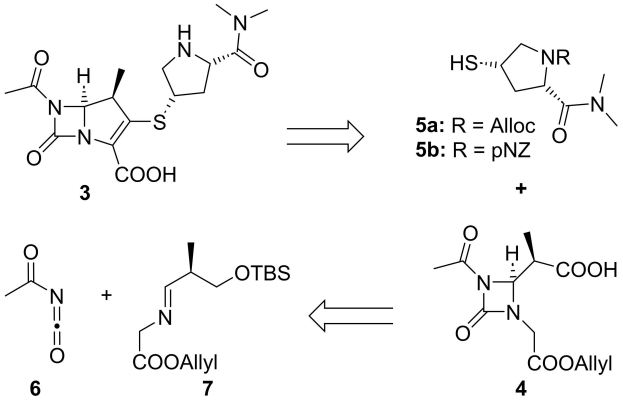

Scheme 2. Global retrosynthesis of meropenem analog **3**. pNZ=*para*-nitrobenzyloxycarbonyl.

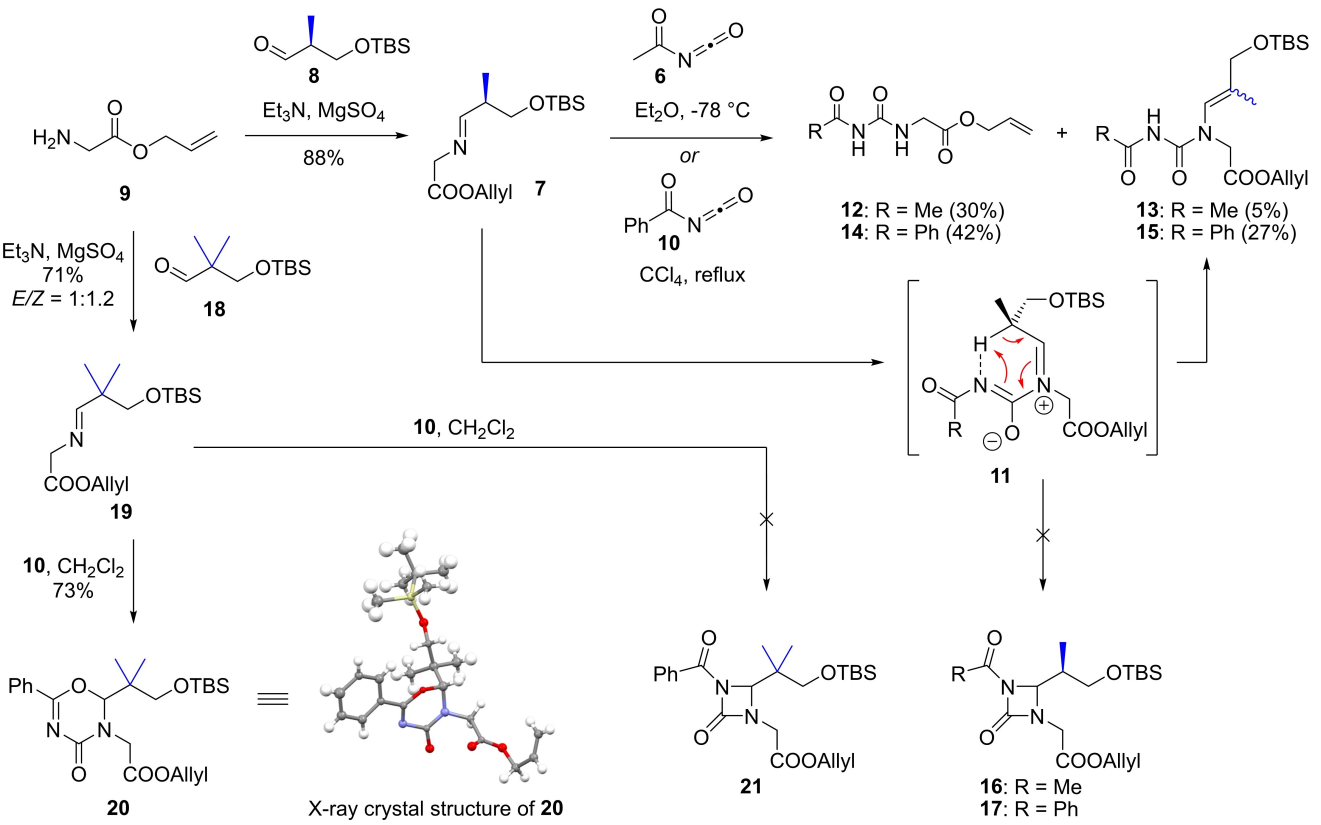

Scheme 3. Reactions of acyl isocyanates with imine **7**.[31,32]

reaction with the isocyanates. (2) Alternatively, amine **9** could be released either from imine **7** or from putative intermediates **11** by reaction with either residual acetamide from the *in situ* preparation of **6** or with benzamide, which is contained in commercial preparations of **10** (up to 20%). It should be noted, however, that commercial trichloroacetyl isocyanate, which is >95% pure, also gave the corresponding urea product. (3) Finally, ureas **12** and **14** may only be formed upon aqueous work-up through hydrolysis of intermediates **11**.[30] As for the formation of enamides **13** and **15**, we assume that these products arise from proton loss from the initial addition product **11**, possibly through an intramolecular 1,5-proton shift to the original isocyanate nitrogen (Scheme 3).

It is also conceivable, however, that imine isomerization to the enamine precedes nucleophilic attack on the isocyanate or that both mechanisms are operative in parallel. Independent of the operating mechanism, the results of these orientating experiments led us to conclude that imine **7** was not a suitable precursor for the preparation of the desired diazetidinones.

Therefore, we considered it important to investigate the reaction of acyl isocyanates with imines such as **19** (Scheme 3). The latter contains a *gem*-dimethyl group at the imine α-carbon,[33] which excludes isomerization to an enamine and also prevents enamide formation from the initial putative iminium intermediate. With this alternative pathway blocked, we envisioned that diazetidinone formation would become a more favorable reaction pathway. Reaction of aldehyde **18**[34] with amine **9** gave imine **19** in 63% yield as an inseparable 5:1 mixture with **18** (13%) (Scheme 3).

Treatment of this material with trichloroacetyl isocyanate led to a complex mixture of products, including allyl ((2,2,2-trichloroacetyl)carbamoyl)glycinate and aldehyde **18**, along with other unidentified structures. In contrast, when imine **19** was treated with benzoyl isocyanate (**10**), the [4+2]-cycloaddition product **20** was obtained in 73% yield; the corresponding [2+2]-cycloaddition product **21** was not observed.

As discussed in the Introduction, Arbuzov and co-workers have reported competition between [4+2] and [2+2] cycloaddition in the reaction of acyl isocyanates and imines[18,19] with the preferred pathway being dependent on different reaction parameters such as temperature and solvent but also the nature of the imine and the acyl isocyanate. Unfortunately, in our case, changing solvents or temperature never led to formation of the desired 1,3-diazetidinone. Although disappointing, our observations are in line with the fact that four-membered ring formation has only been reported for reactions of acyl isocyanates with imines derived from (substituted) benzaldehydes.[18,19] It should also be noted that the spectroscopic discrimination between potential four- and six-membered ring products was challenging. For a given reaction, both types of products exhibit the same molecular mass and contain only few hydrogen atoms in the heterocyclic core, thus making analysis by ^{1}H or standard 2D NMR spectroscopy difficult; furthermore, no reference values for ^{13}C NMR shifts are available

in the literature for either type of structure. ^{15}N NMR spectroscopy was inconclusive and, likewise, manual assignment of IR vibration frequencies to either an imine or a ketone moiety was ambiguous (in contrast to computational assignment, *vide infra*). Finally, although hampered by the tendency of the compound to decompose, X-ray crystallography unequivocally confirmed the six-membered ring structure of **20**. While the quality of the crystals and their size did not allow the unambiguous assignment of atom types, the presence of a six-membered rather than a four-membered ring could be established.[32]

Trying to build on the insights gained from the experiments of imine **7** with isocyanates, we also investigated the reaction of α,β-unsaturated ester enamine **23** with benzoyl isocyanate (**10**) (Scheme 4). We hypothesized that enamide **24** that would be formed in this reaction could be induced to undergo intramolecular 1,4-addition to form a diazetidinone ring. (The use of racemic *n*-butyl ester aldehyde **22** rather than a shorter chain alkyl ester was solely based on its more straightforward synthesis).[35] Enamine **23** was obtained from ester aldehyde **22** by reaction with amine **9** under the same conditions as those employed for the formation of **7**; enamine **23** was obtained as a 1:1.2 mixture of *E*/*Z* isomers in 71% yield (Scheme 4). Simple stirring of **23** with 5 equiv. of benzoyl isocyanate (**10**) in CH_2Cl_2 at room temperature gave enamide **24** in excellent yield (96%) as the *E* isomer exclusively. Unfortunately, however, the compound did not undergo 4-exo-*trig* ring closure to the desired diazetidinone **25** under any of the conditions investigated, including the addition of $BF_3 \cdot OEt_2$ or various Brønsted bases as well as variations in solvent and temperature (see SI for details).

Given the difficulties encountered while targeting the desired 1,3-diazetidinones, we turned our attention to the further elaboration of the obtained 2,3-dihydro-4*H*-1,3,5-oxadiazin-4-ones. Although not within our original target scope, we hypothesized that compounds derived from **20** with its unusual 2,3-dihydro-4*H*-1,3,5-oxadiazin-4-one core might still be reactive with protein nucleophiles and when embedded into the proper structural context might exhibit some β-lactamase inhibitory potential. We thus decided to pursue elaboration of **20** into the meropenem-type dihydro-oxadiazinone **27** (Scheme 5) as an alternative target structure. The synthesis of **27** was to proceed through thioester **26**, which would be elaborated into **27** based on formation of the pyrroline ring *via* Dieckmann-type cyclization according to Kondo and coworkers (in analogy what had been foreseen for the synthesis of **3**).[24]

Thioester **26** was planned to be obtained from **20** by desilylation, oxidation of the resulting primary alcohol to a carboxylic acid, and subsequent thioesterification with **5a** or **5b**. However, while desilylation of **20** with TBAF was straightforward and gave the corresponding free alcohol in 72% yield (**S5**; see SI), the attempted oxidation of the latter to the corresponding aldehyde with DMP or under Swern conditions only led to decomposition (not shown here).

These findings are in line with the observed instability of **20**, which rapidly decomposed even upon storage in the freezer. In light of these observations, no further attempts were made at the conversion of **20** into acid **26**. Rather, an alternative strategy for the synthesis of **27** was devised, where thioester formation was to precede the cycloaddition reaction (Scheme 6).

Thus, acid **28** was obtained from the corresponding aldehyde[36] by Pinnick oxidation followed by thioesterification with thiol **5a** to furnish the corresponding thioester (**S8**; see SI) in excellent overall yield (95%). Thiol **5a** was prepared from *trans*-4-hydroxy-L-proline in 4 steps and 40% overall yield (see SI for details).[37] Oxidative cleavage of the PMB-ether with DDQ followed by Swern oxidation of the ensuing primary alcohol (**S9**; see SI) and condensation of the resulting aldehyde **29** with amine **9** furnished imine **30** in 74% overall yield from **28**. Upon treatment of **30** with 3 equiv. of benzoyl isocyanate (**10**) in CH_2Cl_2, only the [4+2]-cycloaddition product **26** was isolated in 67% yield (as a 7:1 mixture with benzamide); none of the [2+2]-cycloaddition product was observed.

In analogy to Kondo's work on the synthesis of 1-β-methylcarbapenems,[24] sequential treatment of thioester **26** with NaHMDS, TMSCl, $ClP(O)(OPh)_2$ and TBAF was expected to result in 5-membered ring formation *via* Dieckmann-type cyclization followed by enol phosphate formation and re-addition of thiol **5a** to produce **34a** (Scheme 7 and Scheme S1).

Unfortunately, none of the desired cyclization/re-addition product **34a** was observed under these conditions. Likewise,

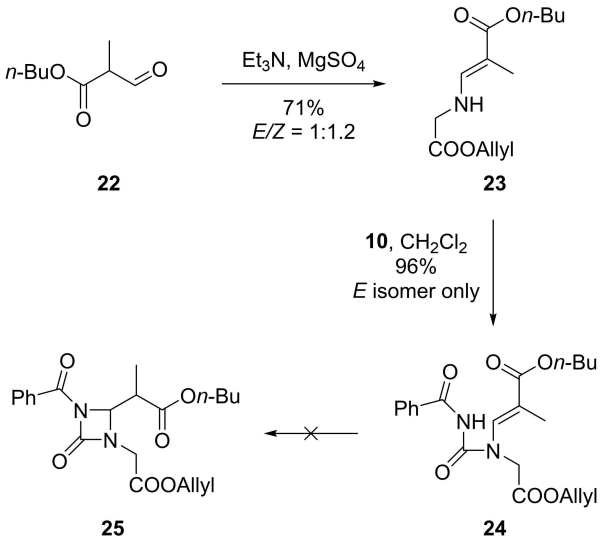

Scheme 4. Attempted synthesis of **25** *via* intramolecular 1,4-addition.

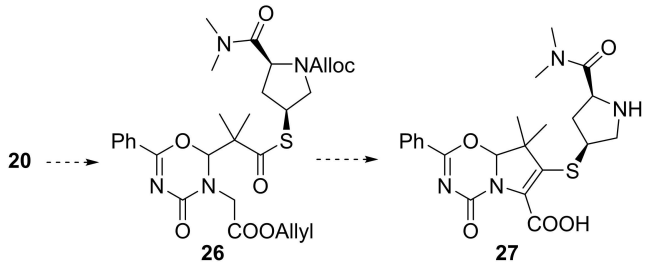

Scheme 5. Structure of meropenem-type dihydro-oxadiazinone **27** envisioned to be accessible from **20** *via* thioester **26**.

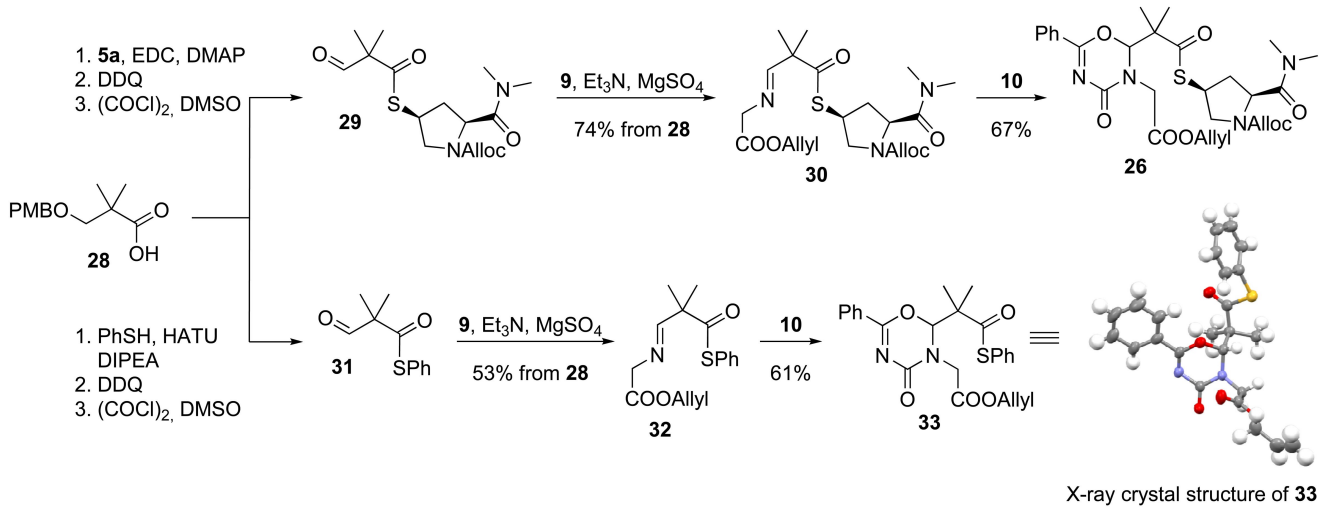

Scheme 6. Synthesis of 2,3-dihydro-4*H*-1,3,5-oxadiazin-4-ones **26** and **33**.[31,38]

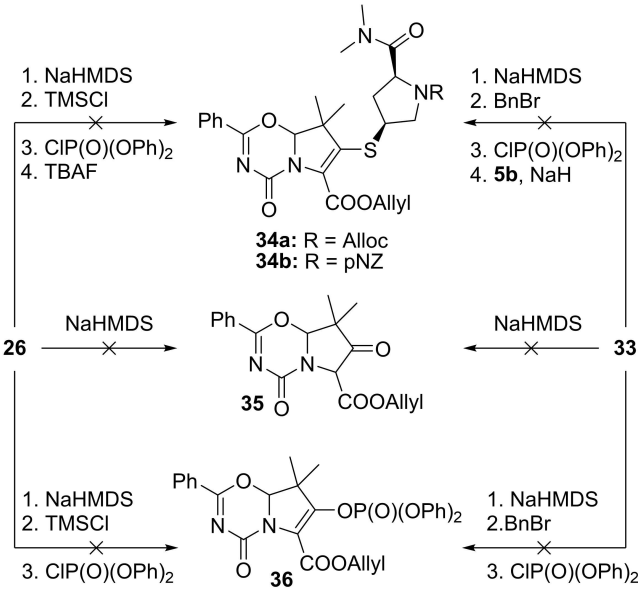

Scheme 7. Dieckmann-type cyclization attempts. pNZ = para-nitrobenzyloxycarbonyl.

attempts to isolate the five-membered ring either as keto ester (**35**) or as enol phosphate (**36**), which could have been further processed into thioenol ether **34**, were unsuccessful (Scheme 7). No Dieckmann cyclization product was observed under any of theconditions investigated (see Table S2 in the SI). The only identifiable products isolated from these reactions were thiol **5a** and the corresponding thiophosphate (**S10**; see SI) both in ca. 15–35% yield.

To investigate if a better thiol leaving group would enable Dieckmann cyclization, phenyl thioester-containing imine **32** was prepared from acid **28** in analogy to the synthesis of **26**. Reaction of **32** with benzoyl isocyanate (**10**) gave 2,3-dihydro-4*H*-1,3,5-oxadiazin-4-one **33** in 31% overall yield from **28** (Scheme 6). Gratifyingly, in contrast to **20**, X-ray crystallography unequivocally confirmed the molecular structure of **33**, including the assignment of all atom types.[38] Interestingly, in contrast to **10**, trichloroacetyl or (mono)chloroacetyl isocyanate did not undergo cycloaddition under identical conditions. Unfortunately, like **26**, thioester **33** could not be converted into **34b**, **35** or **36** (Scheme 7). The corresponding reactions only returned starting material **33** either alone (27%) or as mixture with imine **32**, the corresponding aldehyde and benzyl phenyl sulfide (see Table S3 in the SI).

In light of the complete absence of [2+2] cycloaddition products from the reactions of imines **19**, **30** and **32** with acyl isocyanates, we turned towards the evaluation of the reaction of imine **32** with simple aryl isocyanates that lack the carbonyl group between the aryl and the isocyanate moieties, thereby rendering the undesired [4+2] pathway impossible (Scheme 8). The preparation of 1,3-diazetidinones from phenyl isocyanate and 1,2-bis-(benzylidene-amino)ethane[39] or heterocyclic formamidines,[40] respectively, has been reported previously. However, as for the reactions of acyl isocyanates with imines, we are not aware of any reports on the reactions of phenyl isocyanate with imines derived from aliphatic aldehydes.

In initial experiments, no reaction was observed upon treatment of imine **32** with 5 equiv. of phenyl isocyanate at −78 °C to rt in CH_2Cl_2, Et_2O or MeCN. However, when using 5 equiv. of phenyl isocyanate (**36**) neat, traces of a new product with the desired mass appeared and the same observation was made at 70 °C in CCl_4. Upon further variation of reaction conditions, it was found that the reaction of **37** with 5 equiv. of neat **41** at 70–80 °C yielded 5,5-dimethyl dihydropyrimidine-2,4-dione **42** in 58% yield, rather than the desired diazetidinone (Scheme 8). The outcome of the cycloaddition reaction was independent of the electron-donating/-withdrawing properties of a *para* substituent on the aryl group. Similar yields of **42**, **43** and **44** were obtained for the reaction of **32** with phenyl isocyanate (**37**), *p*-methoxyphenyl isocyanate (**38**), or *p*-nitrophenyl isocyanate (**39**), respectively, under identical conditions (58–64%) (Scheme 8).

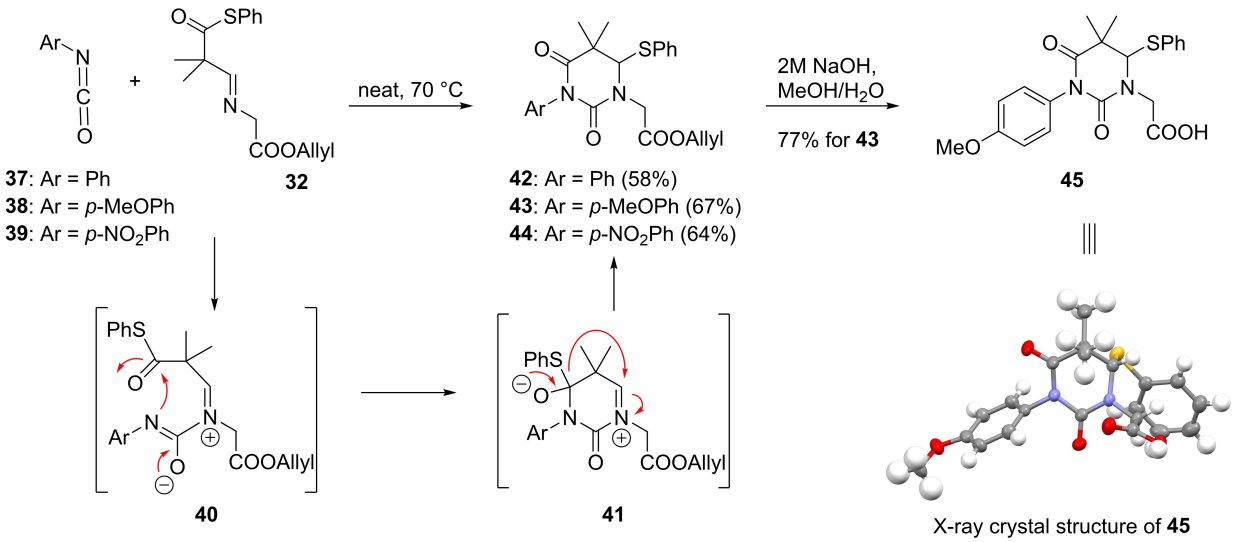

Scheme 8. Synthesis of 5,5-dimethyldihydropyrimidine-2,4-diones **42**–**45**.

The structure of **43** was unequivocally established by X-ray crystallography of the derived acid **45**, which was obtained from **43** by treatment with NaOH/MeOH. In accordance with the formation of **43** from **32** and *p*-methoxyphenyl isocyanate (**38**), reaction of the latter with imine **30** (neat at 70 °C) gave 5,5-dimethyldihydropyrimidine-2,4-dione **46** in 67% yield (Figure 2). Importantly, the reaction of imine **32** and benzyl isocyanate (**47**) furnished **48** in 59% yield (Figure 2), thus indicating that the formation of 5,5-dimethyldihydropyrimidine-2,4-diones from imines and isocyanates is not limited to aryl isocyanates.

A possible mechanism for the formation of 5,5-dimethyldihydropyrimidine-2,4-diones from imines **30**/**32** and aryl isocyanates **37**–**39** or benzyl isocyanate (**47**) is depicted in Scheme 8. After formation of zwitterionic intermediate **40**, the former isocyanate nitrogen attacks the thioester group to form six-membered *S*,*O*-hemiacetal **41**. The latter collapses with re-formation of the carbonyl group and ejection of a thiolate anion, which adds to the iminium moiety to give the final 5,5-dimethyldihydropyrimidine-2,4-dione. Whether the reaction takes place concerted or in a stepwise fashion would need to be determined.

The final conditions elaborated for the reactions of imines **30** and **32** with aryl isocyanates (neat at 70 °C, Scheme 8) were subsequently also applied to the reaction of **32** with benzoyl isocyanate (**10**), which had previously been conducted at 0 °C in CH_2Cl_2 and produced **33** in 61% yield (Scheme 6). No significant change in reaction outcome was observed if **32** was reacted neat with **10** either at room temperature or at 70 °C; **33** was obtained as the major product in both cases (41% yield and 54% yield, respectively). Again, no formation of the four-membered ring product was observed.

Finally, in order to determine if [2+2] cycloaddition may occur between aryl isocyanates and imines that do not incorporate a thioester group, we investigated the reaction of isocyanates **37**–**39** with imine **49** (Figure 3).

However, in no case did heating of imine **49** with isocyanates to 80 °C either neat or in CCl_4 or ClC_2H_4Cl as solvents result in any conversion (based on reaction monitoring by ^{1}H NMR spectroscopy). When the temperature was raised to 200 °C, decomposition was predominant and up to 21% of the aldehyde component of the imine could be isolated next to unidentified side products.

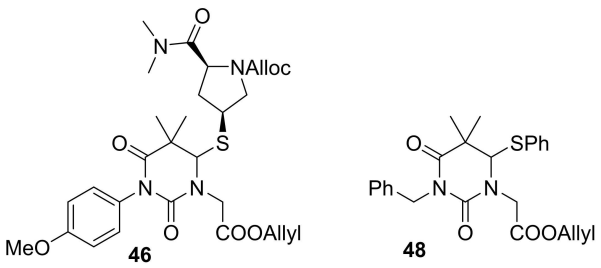

Figure 2. Products obtained from reactions of imine **30** with *p*-methoxyphenyl isocyanate (**38**) (**46**) and of imine **32** with benzyl isocyanate (**47**) (**48**).

DFT Calculations

To rationalize our experimental findings and support proposed mechanisms, we studied the reactions between benzoyl isocyanate (**10**) and imines **19** or **32**, respectively (Scheme 9, reactions A and B), using DFT calculations. By locating all stationary points of the proposed mechanism, we can compare the barrier heights and relative product stabilities.[41] For

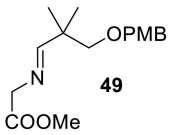

Figure 3. Structure of imine **49**.[31]

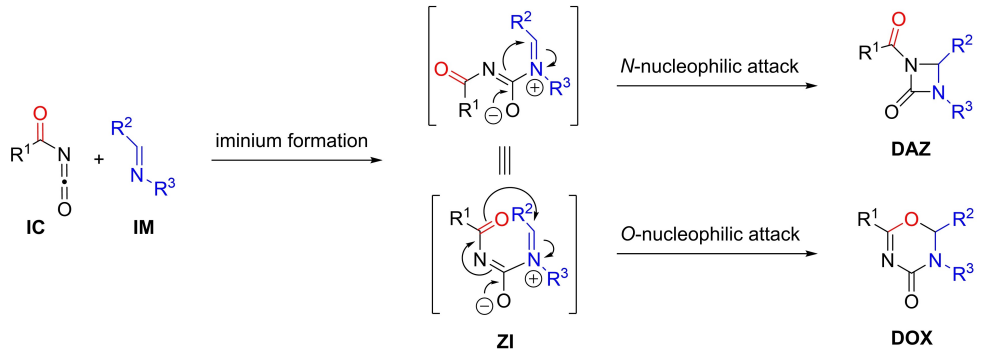

Reaction A: IC = **10**, IM = **19** (*cf.* Scheme 3)
Reaction B: IC = **10**, IM = **32** (*cf.* Scheme 6)
Reaction C: IC = **50**, IM = **51** (R^1 = CCl_3; R^2 = *p*-(Me_2N)Ph; R^3 = Ph)
Reaction D: IC = **10**, IM = **51** (R^1 = Ph; R^2 = *p*-(Me_2N)Ph; R^3 = Ph)

Scheme 9. Mechanistic hypotheses considered for reactions A–D. Reactions A and B produced dihydro-oxadiazinones DOX and no 1,3-diazetidinones DAZ, while reactions C and D were reported by Arbuzov[18,19] to give mixtures of DAZ and DOX.

comparison, we also included the reactions of N-[4-(dimethylamino)benzylidene]aniline (**51**) with trichloroacetyl isocyanate (**50**) and with benzoyl isocyanate (**10**) (Scheme 9, reactions C and D), which have been reported previously by Arbuzov and co-workers.[18,19] Reactions A and B were selected because they had both furnished the respective dihydro-oxadiazinones **20** and **33** as the major products (73% and 61% yield, respectively), which greatly simplified the computational setup.

Reactions C and D were chosen because among all examples reported by Arbuzov, they provided the highest levels of four-membered ring formation. It is noteworthy, however, that even for the reactions of imine **51** with either **10** or **50**, formation of the six-membered ring product was competitive and could be the chief reaction pathway, depending on reaction conditions.

In the proposed mechanism, isocyanates (IC) and imines (IM) react to form an intermediate zwitterionic iminium species (ZI). *N*-Centered or *O*-centered nucleophilic attack then yields N(3)-acyl-1,3-diazetidinones (DAZ) or 2,3-dihydro-4*H*-1,3,5-oxadiazin-4-ones (DOX), respectively (Scheme 9).

Given the relative size, number of rotatable bonds, and possibly shallow potential energy surface of the reactions investigated, we anticipated the importance of rigorous conformational sampling of all species, including transition state structures. Accordingly, we set up a computational pipeline using autodE v.1.3.2[42] with xtb/6.5.1[43] as *lmethod* and ORCA/5.0.3[44,45] as *hmethod*. This workflow was recently reported to perform well on a large array of organic and inorganic reaction classes,[42] including examples with multiple low-energy conformers. Default values were used for DFT-related parameters defined by autodE except for the optimization convergence criterion, which was set to TightOpt. Furthermore, pruning of small-ring transition states was deactivated. An example Python script is provided in the SI. In brief, low energy conformers of reactants were generated with the ETKDG algorithm[46] implemented in RDKit v.2022.09.1.[47] Resulting conformers were optimized using xtb v.6.5.1 (GFN2-xTB Hamiltonian)[48] followed by ORCA v.5.0.3[44] on the PBE0/def2-SVP[49–51] level of theory with the RIJCOSX[52] approximation. Dispersion interactions were included using the D3 correction[53] with Becke-Johnson damping.[54] Solvation effects were included using CPCM[55] (ORCA) and the GBSA model[56] (xtb) with parameters appropriate for dichloromethane. Transition state candidates were located *via* a constrained optimization of initial guesses generated by an adaptive path search algorithm at the same level of theory.[57] Transition state conformers were generated using a randomize and relax algorithm[42] and optimized at the same level of theory. We subsequently performed frequency calculations on the converged structures of all stationary points to confirm true minima (no imaginary frequencies). True transition states were confirmed through the presence of one strong imaginary mode connecting product and starting material.[58] For final single point calculations on all stationary points, the basis set was expanded to def2-TZVP.[51] Gibbs free energies were estimated using scaled frequencies[59] (λ_{harm} = 0.96) and the quasi-RRHO approach.[60] We simulated multiple replicates of each run to account for stochastic processes in the pipeline (e.g. conformer generation) and report average results. Using this approach, we successfully localized the relevant stationary points for all four reactions. Figure 4 shows the resulting energy profiles for reactions A and C (for the energy profiles of reactions B and D and transition state structures for all four reactions, see the SI; Figures S8 and S9. Coordinate files of all stationary points are also provided in the SI).

Relative product stability of four-membered **DAZ-A** (i.e. **21**, Scheme 3) versus six-membered **DOX-A** (i.e. **20**, Scheme 3) was found to differ by around 1.1 kcal/mol. However, the barrier heights for transition state **TS-II-A** leading to **DAZ-A** was found to be 13.4 kcal/mol higher than the corresponding barrier of **TS-III-A** leading to **DOX-A**. This finding is consistent with our observation that reaction A exclusively yielded **DOX-A** but no diazetidinone. In contrast, the corresponding barrier heights for reaction C differ by only 1.5 kcal/mol (13.1 *vs.* 11.6 kcal/mol),

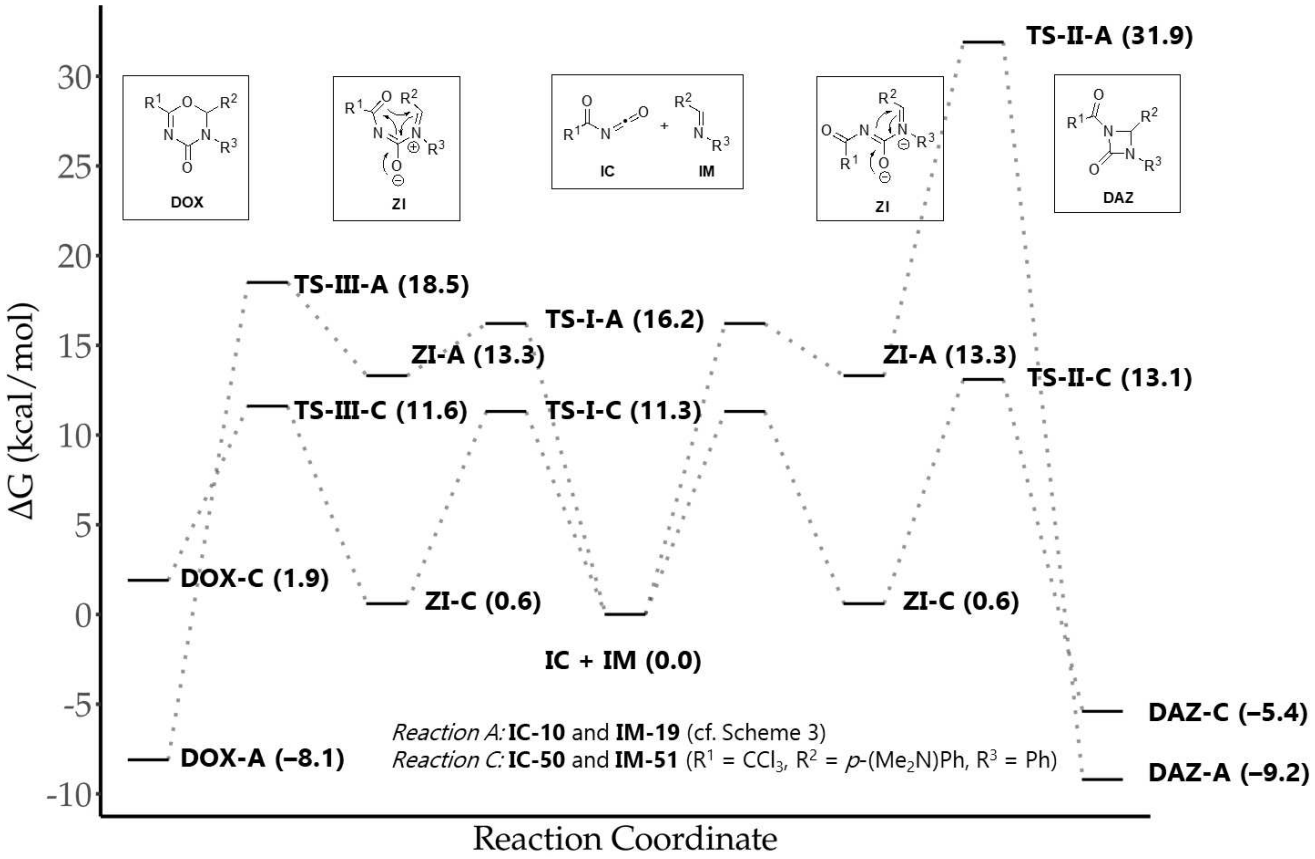

Figure 4. Reaction energy profiles for reactions A and C on the PBE0/def2-TZVP(D3BJ)-CPCM(dichloromethane) level of theory. The educt state isocyanate (IC) and imine (IM) is shown in the middle. The first step of the reaction (iminium formation, ZI) is the same for both directions. Subsequent *N*-centered nucleophilic attack to yield 4-membered ring DAZ is shown on the right, whereas *O*-centered nucleophilic attack to yield six-membered ring DOX is shown on the left. Gibbs free energies are provided in parentheses and are average values over four independent runs and reported relative to the respective starting materials IC and IM. The plot was visualized using EveRplot v.1.3.[61] **DAZ-A** (**21**)/**DAZ-C** and **DOX-A** (**20**)/**DOX-C** refer to the 1,3-diazetidinones and dihydro-oxadiazinones, respectively, from reactions A and C. For transition state structures cf. Figure S8.

slightly favoring formation of **DOX-C**. Relative product stability, on the other hand, favors the formation of **DAZ-C** by 7.3 kcal/mol. These results are consistent with reports by Arbuzov[18,19] who observed product mixtures for reaction C, with product ratios DAZ/DOX depending on solvent and temperature. Such changes in reaction parameters are expected to shift the free potential energy surface, with certain conditions favoring the formation of **DAZ-C** over **DOX-C** and *vice versa*. It is also conceivable that higher temperature might lead to thermodynamic product control over kinetic product control that we hypothesize is dominant at lower temperatures. Similar conclusions were derived for reactions B and D (see SI).

While the barrier height for **TS-II-B** is 14.9 kcal/mol higher than for **TS-III-B**, the corresponding difference for reaction D is only 7.2 kcal/mol, suggesting that competitive reaction pathways could be operative for different reaction conditions. These computational results help rationalize why our attempts to access N(3)-acyl 1,3-diazetidinones *via* the reaction of acyl isocyanates with imines **19**, **30**, or **32** have remained unsuccessful. At the same time, they support the proposed mechanism outlined in Scheme 9, which might enable future improvements in this class of reactions.

Automatic IR Alignments

As alluded to earlier, it was not possible to unequivocally differentiate between DAZ and DOX products by means of ^{1}H and ^{13}C NMR spectroscopy due to the small number of NMR active atoms in the relevant regions of the molecules. Furthermore, the use of X-ray diffraction was limited by the availability of suitable crystals, which prevented routine assignment of reaction products. In light of these difficulties, we were interested whether a distinction between DAZ and DOX products was possible with our recently published computational workflow that relies on alignment of experimentally recorded IR spectra with theoretically predicted reference spectra of candidate structures.[62–64] The IRSA algorithm takes the random error of theory into account alongside the experimental peak pattern. The workflow results in unbiased alignment scores that correlate with the probability of a correct match. This protocol has been successfully applied to differentiate configurational as well as constitutional isomers of a broad variety of molecules.[62–64]

Theoretical reference spectra of structures **DAZ-A** (i.e. **21**) and **DOX-A** (i.e. **20**) (Figure 5) were obtained using a modified version of the procedure described in ref (64). In brief,

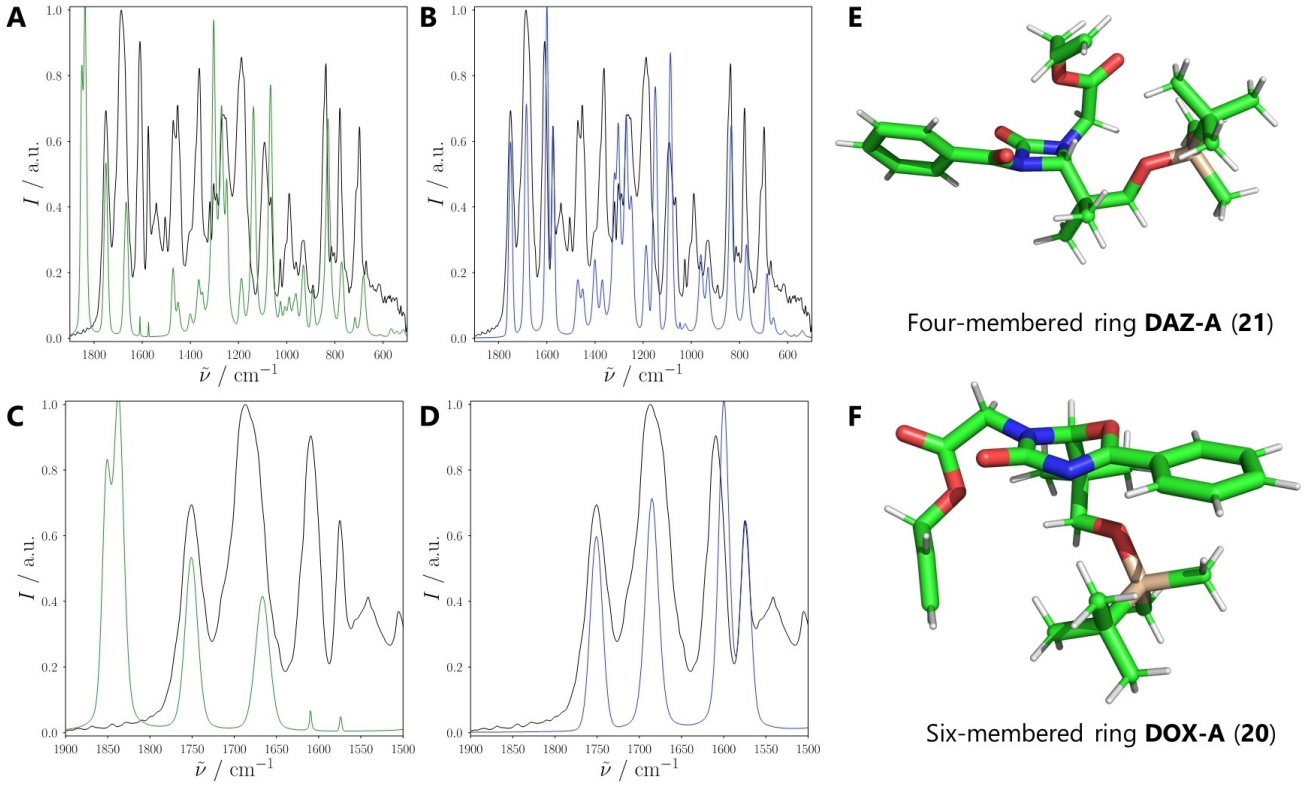

Figure 5. (A, B) IRSA-aligned theoretical spectra for four-membered **DAZ-A** (**21**) (green) and six-membered **DOX-A** (**20**) (blue) together with the experimentally recorded IR spectrum of **20** (black). Alignment of the experimental spectrum with the theoretical spectrum of structure **DAZ-A** yields a Pearson coefficient $r_P = 0.01$ and Spearman coefficient $r_S = 0.13$. Corresponding values for alignment with the theoretical spectrum of **DOX-A** are $r_P = 0.19$ and $r_S = 0.38$. Inlets (C, D) of the range 1900–1500 cm^{-1} region. Further shown are low-energy conformers for **DAZ-A** (E) and **DOX-A** (F).

conformers were generated using the ETKDG algorithm,[46] optimized with MMFF94 s,[65,66] and clustered using the Butina algorithm[67] as implemented in RDKit v.2022.09.1.[47] Resulting cluster centroids were geometry pre-optimized at the RI-BP86/def2-SVP(D3BJ)[51,53,54,68,69] level of theory using ORCA/5.0.3.[44,45] Geometry pre-optimized conformers were clustered again, and remaining centroids optimized with the def2-TZVP basis set followed by frequency calculation at the same level of theory. Theoretical spectra of remaining cluster centroids were Boltzmann-weighted based on their estimated Gibbs free energy (*vide supra*) and broadened assuming a Lorenz shape and a bandwidth of 12 cm^{-1} to give theoretical references. The theoretical spectra were aligned using the published IRSA package (https://github.com/rinikerlab/irsa) in the range 1900–500 cm^{-1}. Figures 5A and B show aligned reference spectra of **DAZ-A** and **DOX-A** next to the experimental spectrum of **20**.[70]

The theoretical reference spectrum of dihydro-oxadiazinone **DOX-A** matches the overall peak shape of the experimental spectrum of the product obtained from the reaction of benzoyl isocyanate (**10**) and imine **19** (Figure 5B).

Especially the vibrational modes between 1900–1500 cm^{-1} (Figure 5D) are explained very well by the theoretical spectrum. In contrast, the theoretical reference spectrum calculated for diazetidinone **DAZ-A** matches the experimental spectrum poorly (Figures 5A and C). These ostensible differences are captured quantitatively in the Pearson and Spearman correlation coefficients r_P and r_S. While the spectrum calculated for **DOX-A** has relatively high correlation scores of 0.19 and 0.38, the corresponding coefficients are 0.01 and 0.13 for the spectrum calculated for **DAZ-A**. These findings clearly illustrate that our workflow allows the reliable distinction between DAZ and DOX products on the basis of IR spectroscopy in conjunction with computational chemistry methods.

Next, we set out to rationalize the major differences in the spectra calculated for possible structural candidates. We visualized the major modes calculated for six-membered candidate **DOX-A** in the 1900–1500 cm^{-1} part of the IR spectrum and found that they correspond to stretching vibrations of the allylic carbonyl group (1740 cm^{-1}) and the carbonyl group of the six-membered ring (DOX) (1670 cm^{-1}), as well as rocking vibrations of the subunit comprised of the heterocyclic core and phenyl side chain (1590 cm^{-1} and 1570 cm^{-1}) (Figure 5D). In contrast, major bands for four-membered **DAZ-A** in the same spectral region correspond to stretching vibrations of the carbonyl group located within the four-membered ring (DAZ) (1830 cm^{-1}) as well as in the exocyclic allyloxycarbonyl (1750 cm^{-1}) and benzoyl groups (1660 cm^{-1}) (Figure 5C). Inspection of the geometries of low-energy conformers for **DAZ-A** and **DOX-A** (Figures 5E and F) revealed that while the exocyclic phenyl group of **DOX-A** is in the same plane as the six-membered ring (Figure 5F), the exocyclic benzoyl group in **DAZ-A** is out of the plane defined

by the four-membered ring (Figure 5E). These differences in geometry suggest the presence of an extended π-system in **DOX-A** that has no correspondence in **DAZ-A**, thus offering an explanation for the presence of the two strong bands around 1600 cm^{-1}, which are absent in the theoretical spectrum of **DAZ-A**. Carbonyl groups incorporated in small rings typically show vibration frequencies at higher wave numbers than those embedded in acyclic chains or medium-sized rings. For example, Arbuzov reported that it was possible to distinguish the formal [2+2] adduct from the formal [4+2] adduct *via* IR band assignment of involved carbonyl groups (1780 cm^{-1} and 1690 cm^{-1} for DAZ *vs.* 1670 cm^{-1} for DOX).[18,19] However, for compounds of increased structural complexity that feature additional carbonyl groups, as in the cases investigated here, and due to the scarcity of literature data for the heterocyclic cores, the magnitude of the shift was difficult to predict *a priori* without a theoretical reference. In contrast, the presented IRSA method provides a simple way to gauge experimental data against theoretical references in an unbiased way, thus aiding the structural elucidation of complex substrates.

Conclusions

This work was originally motivated by the question whether the [2+2] cycloaddition of acyl isocyanates with functionalized imines would constitute a suitable path towards the synthesis of N(3)-acyl-1,3-azetidinone-based analogs **2** of classical β-lactam antibiotics. While the reaction of acyl isocyanates with imines derived from aromatic aldehydes and anilines has been studied in the past, their reaction with functionalized, non-aromatic imines, to the best of our knowledge, has not been investigated. Unfortunately, the projected [2+2] cycloadditions *en route* to **2** were not observed, at least for those pairs of isocyanates and functionalized imines that we have investigated here. While α-monosubstituted imines underwent neither [2+2] nor [4+2] cycloaddition, [4+2] cycloaddition did occur with α,α-disubstituted imines. These findings are in agreement with results of DFT calculations, which showed a large difference between the activation barriers for the formation of a 1,3-diazetidinone (DAZ) and a 2,3-dihydro-1,3,5-oxadiazin-4-one (DOX) ring from a common zwitterionic iminium intermediate (ZI). In contrast, this difference in energy barriers was found to be significantly smaller for an acyl isocyanate/imine pair that had been reported previously to undergo [2+2] cycloaddition under appropriate experimental conditions.

While the six-membered ring structure of the cycloaddition products **20** and **33** could ultimately be assigned on the basis of X-ray crystallography, we could also show that the automated alignment of theoretical and experimental IR spectra by means of the recently developed IRSA algorithm provides an efficient approach to distinguish between 1,3-diazetidinone- and 2,3-dihydro-4*H*-1,3,5-oxadiazin-4-one-derived structures.

Intriguingly, the reactions of imines bearing a thioester moiety in the 2-position with aryl isocyanates or benzyl isocyanate gave neither 1,3-diazetidinones nor dihydro-oxadiazinones; rather, these reactions produced 5,5-dimethyl-6-(aryl-/alkylthio)-dihydropyrimidine-2,4-diones in good yields. The reaction most likely follows an alternative [4+2] cycloaddition pathway, with displacement of the thiol component of the ester in the ring-closing step followed by addition of the thiol to the iminium moiety.

In summary, the work described here provides new insights into the reaction of isocyanates with imines, even though the envisaged 1,3-diazetidinones were not observed. Of particular note, 6-(aryl-/alkylthio)-dihydropyrimidine-2,4-diones, such as **42**–**44**, **46** and **48**, to the best of our knowledge, have not been reported in the literature but may be of interest as intermediates in the synthesis of new bioactive heterocycles.

Supporting Information

The Supporting Information contains all experimental details, NMR spectra, crystallographic data, reaction profiles for reactions B and D and unaligned reference IR spectra. It also includes two zip files with (1) the coordinates of all stationary points in the calculation of reaction profiles and an example script and (2) theoretical IR spectra and coordinates of conformers used in the calculations. Additional references cited within the Supporting Information.[71–76]

Acknowledgements

Institutional support by the ETH Zurich is gratefully acknowledged (K. -H. A., S. R.). We are indebted to Dr. Bernhard Pfeiffer and Dr. Philipp Waser (ETHZ) for NMR support, to Kurt Hauenstein (ETHZ) for technical advice and to Louis Bertschi, Michael Meier, and Daniel Wirz (ETHZ) for HRMS spectra acquisition. We are grateful to Dr. Nils Trapp and Michael Solar (ETHZ) for solving the X-ray crystal structures of compound **S4**, **12**, **14**, **S9**, **20**, **33** and **45**. Dr. Lennard Böselt and Paul Katzberger (ETHZ) are acknowledged for helpful discussions regarding the IRSA algorithm and reviewing the manuscript, respectively. We thank Michael Bogdos (ETHZ) for granting access to and providing assistance with an early version of EveRplot. Open Access funding provided by Eidgenössische Technische Hochschule Zürich.

Conflict of Interests

The authors declare no conflict of interest.

Data Availability Statement

The data that support the findings of this study are available in the supplementary material of this article or upon request from the authors.

Keywords: diazetidinones · isocyanates · reaction mechanisms · IR spectra alignment (IRSA) algorithm · dihydro-oxadiazinones

[1] R. Laxminarayan, *Lancet* **2022**, *399*, 606–607.
[2] C. Mattar, S. Edwards, E. Baraldi, J. Hood, *Curr. Opin. Microbiol.* **2020**, *57*, 56–61.
[3] CDC. Antibiotic Resistance Threats in the United States, 2019. Atlanta, GA: U.S. Department of Health and Human Services, CDC; **2019**. https://www.cdc.gov/drugresistance/Biggest-Threats.html.
[4] C. T. Walsh, T. A. Wencewicz, *J. Antibiot.* **2014**, *67*, 7–22.
[5] For a recent analysis of the global preclinical antibiotics pipeline, see: Theuretzbacher, K. Outterson, A. Engel, A. Karlén, *Nat. Rev. Microbiol.* **2019**, *18*, 275–285.
[6] For a recent review on penicillin-binding proteins and their inhibition by β-lactam antibiotics, see: Mora-Ochomogo, C. T. Lohans, *RSC Med. Chem.* **2021**, *12*, 1623–1639.
[7] For a recent review on β-lactamase inhibitors, see: R. Li, X. Chen, C. Zhou, Q.-Q. Dai, L. Yang, *Eur. J. Med. Chem.* **2022**, *242*, 114677.
[8] D. E. Ehmann, H. Jahić, P. L. Ross, R.-F. Gu, J. Hu, G. Kern, G. K. Walkup, S. L. Fisher, *Proc. Natl. Acad. Sci. USA* **2012**, *109*, 11663–11668.
[9] D. E. Ehmann, H. Jahić, P. L. Ross, R.-F. Gu, J. Hu, G. Kern, T. F. Durand-Réville, S. Lahiri, J. Thresher, S. Livchak, N. Gao, T. Palmer, G. K. Walkup, S. L. Fisher, *J. Biol. Chem.* **2013**, *288*, 27960–17971.
[10] A. Nangia, P. S. Chandrakala, M. V. Balaramakrishna, T. V. A. Latha, *J. Mol. Struct.* **1995**, *343*, 157–165.
[11] A. Nangia, *J. Mol. Struct.* **1991**, *251*, 237–243.
[12] A. Nangia, *Proc. Indian Acad. Sci. Chem. Sci.* **1993**, *105*, 131–139.
[13] M. Coll, J. Frau, B. Vilanova, J. Donoso, F. Munoz, F. G. Blanco, *J. Phys. Chem. B* **2000**, *104*, 11389–11394.
[14] M. Coll, J. Frau, B. Vilanova, J. Donoso, F. Muñoz, *J. Comput.-Aided Mol. Des.* **2001**, *15*, 819–833.
[15] R. C. Garćas, M. Coll, J. Donoso, F. Muñoz, *Chem. Phys. Lett.* **2003**, *372*, 275–281.
[16] A. Nangia, P. S. Chandrakala, *Tetrahedron Lett.* **1995**, *36*, 7771–7774.
[17] P. S. Chandrakala, A. K. Katz, H. L. Carrell, P. R. Sailaja, A. R. Podile, A. Nangia, G. R. Desiraju, *J. Chem. Soc. Perkin Trans. 1* **1998**, *1998*, 2597–2608.
[18] a) N. N. Zobova, G. N. Rusanov, B. A. Arbuzov, *Bull. Acad. Sci. USSR Div. Chem. Sci. (Engl. Transl.)* **1972**, *21*, 1957–1960; b) Original document in Russian: Izvestiya Akademii Nauk SSSR, *Seriya Khimieheskaya* **1972**, *9*, 2016–2020.
[19] a) B. A. Arbuzov, N. N. Zobova, *Bull. Acad. Sci. USSR Div. Chem. Sci. (Engl. Transl.)* **1973**, *22*, 2542–2543; b) Original document in Russian: Izvestiya Akademii Nauk SSSR, *Seriya Khimieheskaya* **1973**, *11*, 2607–2609.
[20] For a review on cycloaddition reactions with acyl isocyanates, see: B. A. Arbuzov, N. N. Zobova, *Synthesis* **1974**, *1974*, 461–476.
[21] O. Tsuge, T. Hatta, R. Mizuguchi, T. Kobayashi, R. Kanzaki, *Heterocycles* **1996**, *42*, 533–536.
[22] O. Tsuge, M. Tashiro, R. Mizuguchi, S. Kanemasa, *Chem. Pharm. Bull.* **1966**, *14*, 1055–1057.
[23] R. Neidlein, R. Bottler, *Arch. Pharm.* **1969**, *302*, 306–309.
[24] M. Seki, K. Kondo, T. Iwasaki, *J. Chem. Soc. Perkin Trans. 1* **1996**, *1996*, 2851–2856.
[25] E. De Lemos, F. H. Porée, A. Bourin, J. Barbion, E. Agouridas, M. I. Lannou, A. Commerçon, J. F. Betzer, A. Pancrazi, J. Ardisson, *Chem. Eur. J.* **2008**, *14*, 11092–11112.
[26] M. S. Stanley *J. Org. Chem.* **1992**, *57*, 6421–6430.
[27] C. C. Hanna, S. S. Kulkarni, E. E. Watson, B. Premdjee, R. J. Payne, *Chem. Commun.* **2017**, *53*, 5424–5427.
[28] The yields reported for products that could only be obtained as mixtures with another component are true chemical yields. They were calculated based on the molar fraction of the product in the mixture as determined by NMR spectroscopy.
[29] D. Q. Song, N. N. Du, Y. M. Wang, W. Y. He, E. Z. Jiang, S. X. heng, Y. X. Wang, Y. H. Li, Y. P. Wang, X. Li, J.-D. Jiang, *Bioorg. Med. Chem.* **2009**, *17*, 3873–3878.
[30] Based on reaction monitoring by ^{1}H NMR, the ureas were already formed during the reaction. However, we cannot strictly exclude that hydrolysis of **11** occurred in the process of taking samples and/or during NMR acquisition.
[31] Imines **7**, **19**, **30**, **32** and **48** are shown as *E* isomers based on literature precedent for related structures: a) W. Van Brabandt, G. Verniest, D. De Smaele, G. Duvey, N. De Kimpe, *J. Org. Chem.* **2006**, *71*, 7100–7102; b) N. Piens, H. Goossens, D. Hertsen, S. Deketelaere, L. Crul, L. Demeurisse, J. De Moor, E. Van den Broeck, K. Mollet, K. Van Hecke, V. Van Speybroeck, M. D'hooghe, *Chem. Eur. J.* **2017**, *23*, 18002–18009; c) S. A. Shehzadi, A. Saeed, F. Lemière, B. U. W. Maes, K. Abbaspour Tehrani, *Eur. J. Org. Chem.* **2018**, *2018*, 78–88; and based on Nuclear Overhauser Enhancement Spectroscopy (NOESY) for compounds **30**, **32** and **48**.
[32] Due to these limitations, no coordinates for this structure have been deposited in the Cambridge Crystallographic Data Centre (CCDC). Deposition numbers 2290115 (for **S4**), 2290117 (for **12**), 2290124 (for **14**), 2290123 (for **S9**), 2300752 (for **33**) and 2290121 (for **45**) contains the supplementary crystallographic data for this paper. These data are provided free of charge by the joint Cambridge Crystallographic Data Centre and Fachinformationszentrum Karlsruhe Access Structures service.
[33] Carbapenems with *gem*-dimethyl substitution have been reported to exhibit antibiotic activity, although actual data are not included in the corresponding publication. The compounds were simply noted "… [to exhibit] considerable activities against a number of Gram positive and Gram negative organisms": M. Shibuya, S. Kubota, *Tetrahedron Lett.* **1981**, *22*, 3611–3614.
[34] H. Nakatsuji, H. Nishikado, K. Ueno, Y. Tanabe, *Org. Lett.* **2009**, *11*, 4258–4261.
[35] F. Richter, M. Bauer, C. Perez, C. Maichle-Mössmer, M. E. Maier, *J. Org. Chem.* **2002**, *67*, 2474–2480.
[36] T. Trieselmann, R. W. Hoffmann, K. Menzel, *Eur. J. Org. Chem.* **2002**, *2002*, 1292–1304.
[37] Thiol **5a** has been reported in the literature multiple times, but no experimental protocols for the preparation of the compound have been published: a) Ref. [24]; b) O. Sakurai, T. Ogiku, M. Takahashi, M. Hayashi, T. Yamanaka, H. Horikawa, T. Iwasaki, *J. Org. Chem.* **1996**, *61*, 7889–7894; c) M. Seki, K. Kondo, T. Iwasaki, *Synlett* **1995**, *1995*, 315–316; d) K. T. M. Sungawa, A. Sasaki, H. Matsumura, K. Goda, *Chem. Pharm. Bull.* **1994**, *42*, 1381–1387; e) M. Sunagawa, H. Matsumura, A. Sasaki, H. Yamaga, Y. Kitamura, Y. Sumita, H. Nouda, *J. Antibiot.* **1997**, *50*, 621–627.
[38] Crystals of **33** contained two *N*-Alloc conformers in a 9:1 ratio. Only the major conformer is shown in Scheme 6, but an overlay of both conformers is shown in Figure S5 in the SI.
[39] J. Van Alphen, *Recl. Trav. Chim. Pays-Bas* **1935**, *54*, 885–887.
[40] M. Tišler, B. Stanovnik, *J. Chem. Soc. Chem. Commun.* **1980**, *1980*, 313–314.
[41] We also investigated concerted mechanisms that would directly transform starting isocyanates (IC) and imines (IM) into 1,3-diazetidinones (DAZ) or dihydro-oxadiazinones (DOX). However, for all reactions investigated, we were unable to locate a corresponding transition state (results not shown). This finding, in conjunction with other products of related reactions that can be explained *via* a common zwitterionic iminium intermediate (ZI) (for example those shown in Scheme 8) led us to focus on a step-wise reaction mechanism.
[42] T. A. Young, J. J. Silcock, A. J. Sterling, F. Duarte, *Angew. Chem. Int. Ed.* **2021**, *60*, 4266–4274.
[43] C. Bannwarth, E. Caldeweyher, S. Ehlert, A. Hansen, P. Pracht, J. Seibert, S. Spicher, S. Grimme, *Wiley Interdiscip. Rev.: Comput. Mol. Sci.* **2021**, *11*, e1493.
[44] F. Neese, F. Wennmohs, U. Becker, C. Riplinger, *J. Chem. Phys.* **2020**, *152*, 224108.
[45] F. Neese, *Wiley Interdiscip. Rev.: Comput. Mol. Sci.* **2022**, *12*, e1606.
[46] S. Riniker, G. A. Landrum, *J. Chem. Inf. Model.* **2015**, *55*, 2562–2574.
[47] G. Landrum, P. Tosco, B. Kelley, Ric, sriniker, gedeck, D. Cosgrove, R. Vianello, N. Schneider, E. Kawashima, D. N. A. Dalke, G. Jones, B. Cole, M. Swain, S. Turk, AlexanderSavelyev, A. Vaucher, M. Wójcikowski, I. Take, D. Probst, V. F. Scalfani, K. Ujihara, guillaume godin, A. Pahl, F. Berenger, J. L. Varjo, *Zenodo* **2023**, *7671152*, 1. RDKit (Q3 2022) Release.
[48] C. Bannwarth, S. Ehlert, S. Grimme, *J. Chem. Theory Comput.* **2019**, *15*, 1652–1671.
[49] J. P. Perdew, K. Burke, M. Ernzerhof, *Phys. Rev. Lett.* **1996**, *77*, 3865.
[50] V. Barone, M. Cossi, *J. Phys. Chem. A* **1998**, *102*, 1995–2001.
[51] C. Adamo, V. Barone, *J. Chem. Phys.* **1999**, *110*, 6158–6170.
[52] F. Weigend, R. Ahlrichs, *Phys. Chem. Chem. Phys.* **2005**, *7*, 3297–3305.
[53] F. Neese, F. Wennmohs, A. Hansen, U. Becker, *Chem. Phys.* **2009**, *356*, 98–109.
[54] S. Grimme, J. Antony, S. Ehrlich, H. Krieg, *J. Chem. Phys.* **2010**, *132*, 154104.
[55] S. Grimme, S. Ehrlich, L. Goerigk, *J. Comput. Chem.* **2011**, *32*, 1456–1465.
[56] W. C. Still, A. Tempczyk, R. C. Hawley, T. Hendrickson, *J. Am. Chem. Soc.* **1990**, *112*, 6127–6129.

[57] Consult the autodE v.1.0.0b3 changelog online for more information.
[58] autodE uses a threshold of 40 cm^{-1} to consider a mode significant.
[59] M. K. Kesharwani, B. Brauer, J. M. L. Martin, *J. Phys. Chem. A* **2015**, *119*, 1701–1714.
[60] S. Grimme, *Chem. Eur. J.* **2012**, *18*, 9955–9964.
[61] M. K. Bogdos, B. Morandi, *J. Chem. Educ.* **2023**, *100*, 3641–3644.
[62] L. Böselt, R. Dötzer, S. Steiner, M. Stritzinger, S. Salzmann, S. Riniker, *Anal. Chem.* **2020**, *92*, 9124–9131.
[63] F. Pultar, M. E. Hansen, S. Wolfrum, L. Böselt, R. Fróis-Martins, S. Bloch, A. G. Kravina, D. Pehlivanoglu, C. Schäffer, S. Leib und Gut-Landmann, S. Riniker, E. M. Carreira, *J. Am. Chem. Soc.* **2021**, *143*, 10389–10402.
[64] L. Böselt, R. Aerts, W. Herrebout, S. Riniker, *Phys. Chem. Chem. Phys.* **2023**, *25*, 2063–2074.
[65] T. A. Halgren, *J. Comput. Chem.* **1996**, *17*, 490–519.
[66] T. A. Halgren, *J. Comput. Chem.* **1999**, *20*, 720–729.
[67] D. Butina, *J. Chem. Inf. Comput. Sci.* **1999**, *39*, 747–750.
[68] M. Feyereisen, G. Fitzgerald, A. Komornicki, *Chem. Phys. Lett.* **1993**, *208*, 359–363.
[69] A. D. Becke, *Phys. Rev. A* **1988**, *38*, 3098.
[70] See SI (Figure S10) for the comparison of experimental data with unaligned theoretical reference spectra. Theoretical reference spectra as well as coordinate files of geometry-optimized structures are provided in the SI.
[71] S. J. Gregson, P. W. Howard, J. A. Hartley, N. A. Brooks, L. J. Adams, T. C. Jenkins, L. R. Kelland, D. E. Thurston, *J. Med. Chem.* **2001**, *44*, 737–748.
[72] G. M. Sheldrick, SADABS. Program for Empirical Absorption Correction of Area Detector Data. Univ. of Göttingen: Göttingen, Germany, **1996**.
[73] G. M. Sheldrick, *Acta Cryst.* **2015**, *A71*, 3–8.
[74] G. M. Sheldrick, *Acta Cryst.* **2008**, *A64*, 112–122.
[75] G. M. Sheldrick, *Acta Cryst.* **2015**, *C71*, 3–8.
[76] O. V. Dolomanov, L. J. Bourhis, R. J. Gildea, J. A. K. Howard, H. J. Puschmann, *Appl. Cryst.* **2009**, *42*, 339–341.

Manuscript received: December 21, 2023
Accepted manuscript online: January 16, 2024
Version of record online: January 30, 2024